Perpendicular susceptibility and geometrical frustration in two-dimensional Ising antiferromagnets: Exact solutions

K. A. Muttalib,[1] M. Khatun,[2] and J. H. Barry[1]
[1]*Department of Physics, University of Florida, Gainesville, Florida 32611, USA*
[2]*Department of Physics and Astronomy, Ball State University, Muncie, Indiana 47306, USA*
(Received 16 August 2017; published 9 November 2017)

Discovery of new materials and improved experimental as well as numerical techniques have led to a renewed interest in geometrically frustrated spin systems. However, there are very few exact results available that can provide a benchmark for comparison. In this work, we calculate exactly the perpendicular susceptibility $\chi_\perp$ for an Ising antiferromagnet with (i) nearest-neighbor pair interaction on a kagome lattice where strong frustration prevents long-range ordering and (ii) elementary triplet interactions on a kagome lattice which has no frustration but the system remains disordered down to zero temperature. By comparing with other known exact results with and without frustration, we propose that an appropriately temperature-scaled $\chi_\perp$ can be used as a quantitative measure of the degree of frustration in Ising spin systems.

DOI: 10.1103/PhysRevB.96.184411

I. INTRODUCTION

In a spin system on a lattice, frustration refers to the inability of the spins to satisfy the lowest energy state for each bond, which can result from either competing interactions or the geometry of the lattice, thus inhibiting long-range order. Frustrated spin systems can lead to novel phases like spin glass [1], spin ice [2,3], or spin liquids [4]. Recent discovery of various compounds that show novel effects of frustration [5–8] has led to significant increase in efforts to explore theoretical models that can lead to a better understanding of frustration in both classical and quantum spin systems [9–11].

While many numerical techniques have been developed to understand the properties of various theoretical models like the spin-1/2 Heisenberg model or the asymmetric or extended Hubbard model on a geometrically frustrated lattice [12–26], very few exact results are available which can be used as a qualitative guide or as a quantitative benchmark for comparison. The simplest theoretical model of geometrical frustration is the antiferromagnetic Ising model with nearest-neighbor pair interactions on a two-dimensional triangular lattice, which we will refer to as the triangular Ising antiferromagnet (TIA). The ground state of TIA is highly degenerate, with a finite value of the residual entropy per site at zero temperature given by $S_0^{\rm TIA}/Nk_B = 0.3231\cdots$, where N is the number of lattice sites and k_B is the Boltzmann constant [27,28]. A second theoretical model of geometrical frustration is the antiferromagnetic Ising model on a two-dimensional kagome lattice, shown in Fig. 1, which we will refer to as the kagome Ising antiferromagnet (KIA). Similar to TIA, the ground state of KIA is also highly degenerate, with a zero-temperature residual entropy per site given by $S_0^{\rm KIA}/Nk_B = 0.5018\cdots$, which is larger than that of TIA [29]. This suggests that the ground state of KIA is more frustrated than that of TIA. This is expected since the kagome lattice contains corner-sharing triangles in contrast to edge-sharing ones in the triangular lattice. Both remain disordered down to zero temperature.

The zero-temperature residual entropy is a quantitative measure of the degree of disorder, and in geometrically frustrated systems it can quantify the "degree of frustration" as well. However, in this work we will make a distinction between two types of disorder, with or without frustration, both of which can lead to disordered ground states. We will explore two exactly solvable models that exemplify the two types of disorder and show that the residual entropy does not distinguish between disorder with and without frustration. Alternatively, the temperature dependence of the longitudinal susceptibility $\chi_\parallel(T)$ has been used as an experimentally accessible quantity to characterize disorder with frustration in real physical systems. This phenomenological characterization involves the mean-field (negative) Curie-Weiss transition temperature $\Theta_{\rm CW}$ such that the system behaves like a paramagnet for $T \gg |\Theta_{\rm CW}|$, as well as a "freezing" temperature $T_F \ll |\Theta_{\rm CW}|$ below which the inverse longitudinal susceptibility starts to deviate significantly from a linear behavior, the measure of frustration being given by the ratio [1] $f \equiv -\Theta_{\rm CW}/T_F \gg 1$.

Instead of relying on such a phenomenological characterization, in this work we evaluate the *perpendicular susceptibility* $\chi_\perp(T)$ exactly for two different models: (1) the KIA, which has a high degree of geometric frustration, and (2) a triplet interaction model KIA-T with zero frustration. We emphasize that $\chi_\perp$ involves response to a field perpendicular to the Ising spin axis and hence probes quantum fluctuations. By comparing the results for KIA and KIA-T evaluated in this work with the known exact results for TIA [30] as well as kagome Ising ferromagnet with long-range order [31], we propose that an appropriately temperature-scaled $\chi_\perp$ can be used as a quantitative measure of the degree of geometrical frustration in systems with or without long-range order. The measure suggests that we distinguish between two types of systems that remain disordered down to zero temperature: One is geometrically frustrated as in KIA and TIA, and the other is disordered with no frustration, as in KIA-T. In order to explore the difference between the two types of disordered ground states further, we compare the longitudinal susceptibilities $\chi_\parallel$ for KIA and TIA with that of KIA-T. We find that while frustrated systems have a finite negative Curie-Weiss temperature $\Theta_{\rm CW}$, nonfrustrated KIA-T has $\Theta_{\rm CW} = 0$. In contrast, the residual entropy remains finite in all three models whether or not the disorder arises from frustration.

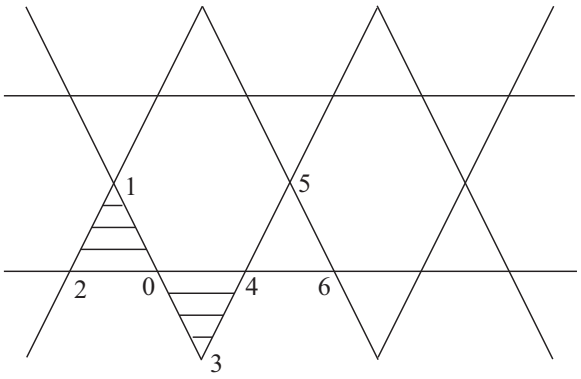

FIG. 1. Kagome lattice. Seven sites are specifically enumerated for use throughout the paper. Lined area is a "bow-tie" unit used in Sec. III.

The remainder of the paper is organized as follows. In Sec. II, we consider the kagome Ising antiferromagnet (KIA) with nearest-neighbor pair interaction and obtain the perpendicular susceptibility exactly for all temperatures using the relevant spin correlations. Although the high-temperature expansion of the parallel susceptibility required for the evaluation of the Curie-Weiss temperature $\Theta_{\rm CW}^{\rm KIA}$ is available [32], we use an alternative method using the pair spin correlations to obtain $\Theta_{\rm CW}^{\rm KIA}$ that agrees with the high-temperature expansion. In Sec. III, we evaluate both perpendicular and parallel susceptibility as well as the entropy exactly at all temperatures for a triplet-interaction model KIA-T. In Sec. IV, we define a parameter that provides a systematic description of the degree of frustration in models with or without long-range order. In Sec. V, we summarize the results and discuss possible future directions.

II. KAGOME ISING ANTIFERROMAGNET WITH PAIR INTERACTION (KIA)

The Hamiltonian of the two-dimensional kagome Ising model with nearest-neighbor pair interactions is given by

$$H_{\rm pair} = -J_2 \sum_{\langle i,j\rangle} \sigma_i^z \sigma_j^z, \tag{2.1}$$

where σ_i^z, σ_j^z are the z-component Pauli spin operators localized on sites i and j of a given lattice, the symbol $\langle i,j\rangle$ representing a sum over all distinct nearest-neighbor pairs, and $J_2 < 0$ is an antiferromagnetic pair-interaction parameter. For a triangular lattice there are six nearest-neighbor sites, while for the kagome lattice there are only four as shown in Fig. 1; both contain elementary triangles that lead to frustration when the interaction is antiferromagnetic. The triangular lattice contains edge-sharing triangles whereas the kagome lattice has corner-sharing triangles. From this geometrical pattern, one expects that KIA is more geometrically frustrated compared to TIA. Next, we calculate the perpendicular susceptibility of KIA as a function of temperature.

A. Perpendicular susceptibility

In the presence of a perpendicular (transverse) magnetic field h_x and associated supplementary Hamiltonian $H_0 = -mh_x \sum_i \sigma_i^x$ where m is the magnetic moment, Ising models are designated *quantum Ising models* since their Hamiltonians contain noncommuting operators and theoretical investigations require use of the Pauli spin algebra. As mentioned earlier, the perpendicular susceptibility $\chi_\perp^{\rm TIA}$ for the triangular Ising antiferromagnet has been calculated exactly by Stephenson [30]. Here we will calculate $\chi_\perp^{\rm KIA}$ for the kagome Ising antiferromagnet exactly on the non-Bravais kagome lattice. Both are models with strong geometrical frustration and both lead to disordered ground states. A comparison will provide us with some insight into the response, to a transverse field, of strongly frustrated systems that do not order down to zero temperature.

In order to calculate $\chi_\perp^{\rm KIA}$ we follow the theoretical techniques introduced in [31], where an exact formula for the zero-field perpendicular susceptibility was obtained for simple quantum Ising models on regular (all sites equivalent, all bonds equivalent) or irregular lattices of arbitrary spatial dimensions. For regular lattices that include triangular and kagome, the *initial isothermal perpendicular susceptibility* per site, $\chi_\perp(T)$, reads [31]

$$\chi_\perp(T) \equiv m \lim_{h_x\to 0} \frac{\partial\langle\sigma_0^x\rangle}{\partial h_x} = m^2\beta\left\langle \frac{\tanh\left[Q_2 \sum_{r'=1}^q \sigma_{r'}^z\right]}{Q_2 \sum_{r'=1}^q \sigma_{r'}^z}\right\rangle. \tag{2.2}$$

Here q is the number of nearest-neighbor sites, the sum is over all nearest neighbors, and we have defined a dimensionless interaction parameter

$$Q_2 \equiv \beta J_2 < 0, \tag{2.3}$$

where $\beta \equiv 1/k_B T$. Since $(\sigma_j^z)^{2n} = 1$, $(\sigma_j^z)^{2n+1} = \sigma_j^z$ for all integers n, it then follows that for kagome ferromagnetic or antiferromagnetic interactions, one can express the *reduced* perpendicular susceptibility as

$$\frac{\chi_\perp^{\rm KIA}}{\chi_2^0} = q|Q_2|[A^+ + 2A^0(x_{01} + x_{05} + x_{06}) + A^- x_{1234}], \tag{2.4}$$

with

$$A^\pm \equiv \frac{1}{8}\left[\frac{\tanh(4Q_2)}{(4Q_2)} \pm 4\frac{\tanh(2Q_2)}{(2Q_2)} + 3\right],$$
$$A^0 \equiv \frac{1}{8}\left[\frac{\tanh(4Q_2)}{(4Q_2)} - 1\right]. \tag{2.5}$$

Here $x_{ij} \equiv \langle\sigma_i^z\sigma_j^z\rangle \equiv \langle ij\rangle$ are the pair spin correlations with $i = 0$ and $j = 1,5,6$, and we have defined the unit of susceptibility in terms of the interaction parameter J_2,

$$\chi_2^0 \equiv \frac{m^2}{q|J_2|}, \tag{2.6}$$

normalized by the lattice coordination number q. The four-spin correlation $x_{1234} \equiv \langle\sigma_1^z\sigma_2^z\sigma_3^z\sigma_4^z\rangle \equiv \langle 1234\rangle$ is the correlation of the nearest-neighbor cluster around site 0 (see Fig. 1 for site labels). The pair correlations have been obtained earlier in [33]; here we obtain the exact solutions for the quartet correlation $\langle 1234\rangle$ using the same techniques developed in [33]. Figure 2 shows the quartet as well as the pair correlations which we include for the sake of comparison and completeness. We also include three additional pair correlations $\langle 15\rangle$, $\langle 16\rangle$, and $\langle 26\rangle$

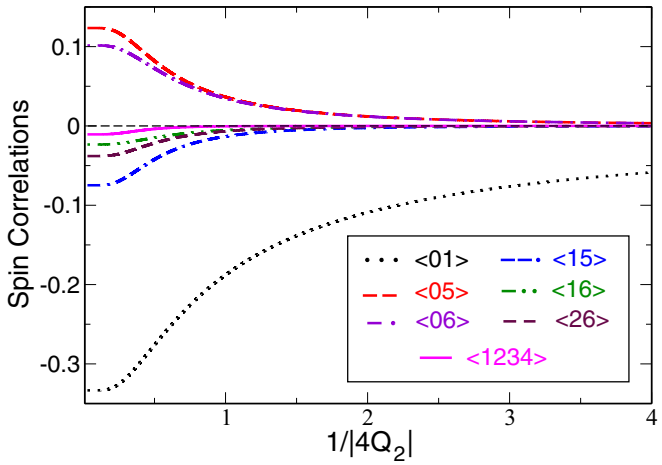

FIG. 2. Exact solution curves of spin correlations for KIA as a function of reduced temperature [Eq. (2.7)], used in the calculation of $\chi_\perp$ in Sec. II A as well as the high-temperature limit of $\chi_\parallel$ in Sec. II B. The four-spin correlation $\langle 1234\rangle$ is shown by the solid (magenta) curve. The pair correlations at distances farther apart decay faster with increasing temperature, with correlations farther than $\langle 15\rangle$ becoming negligible beyond $1/|4Q_2| \gg 2$.

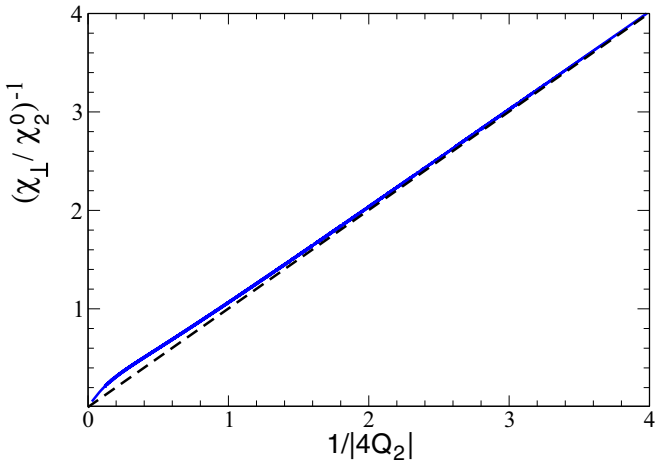

FIG. 3. Inverse of the exact reduced perpendicular susceptibility [Eq. (2.4)] of KIA as a function of reduced temperature [Eq. (2.7)]. The dashed (black) line with slope 1 is the extrapolation from the high-temperature limit. The zero-temperature limit corresponds to a $1/T$ divergence of the perpendicular susceptibility which is similar to TIA [30] and can be considered a signature of geometrically frustrated magnetic systems.

that will be used in our calculation of the high-temperature parallel susceptibility in Sec. II B.

Using the exact spin correlations, we use Eq. (2.4) to obtain $\chi_\perp^{\rm KIA}/\chi_2^0$. Figure 3 shows the exact inverse reduced susceptibility $[\chi_\perp^{\rm KIA}(T)/\chi_2^0]^{-1}$ as a function of *reduced temperature*

$$\frac{1}{|4Q_2|} = \frac{k_B T}{4|J_2|}. \tag{2.7}$$

Comparing with TIA [30], we find that both $\chi_\perp^{\rm KIA}$ and $\chi_\perp^{\rm TIA}$ diverge as $1/T$ as $T \to 0$, but with different amplitudes. As we will argue later, this divergence is a signature of geometrical frustration, the amplitude characterizing the measure of strength or degree of frustration. It is important to note that Fig. 3 contains reduced scales on both axes, such that the high-temperature asymptotic limit of the reduced inverse perpendicular susceptibility as a function of the reduced temperature is a straight line with unit slope that goes through the origin, regardless of the strength of the interaction. (This is different from the inverse parallel susceptibility which has a finite intercept, as will be shown in Sec. II B.) The initial slope is larger than unity, but the undulation that smoothly changes the slope to unity as $T \to \infty$ seems to be a characteristic feature of a frustrated system.

B. Parallel susceptibility

The parallel susceptibility $\chi_\parallel$ for both the kagome (KIA) and the triangular (TIA) lattices have been obtained very precisely using low- and high-temperature expansions by Sykes and Zucker [32]. From the high-temperature expansion of the inverse parallel susceptibility one can extract the Curie-Weiss temperature for both cases as

$$\Theta_{\rm CW} = \frac{q J_2}{k_B}. \tag{2.8}$$

where the lattice coordination number $q = 6$ for TIA and $q = 4$ for KIA.

There exists an alternative method to obtain the parallel susceptibility $\chi_\parallel$. Since $\chi_\parallel$ is a thermodynamic response function, it can be represented in terms of magnetic fluctuations, more particularly for the problem in hand, as an infinite series of solely pair correlations. The fluctuation representation will again be used to obtain $\chi_\parallel$ for the triplet interaction model in Sec. III B. Such representations have the potential to obtain accurate parallel susceptibility for the entire temperature range with only a limited number of pair correlations within a single framework. Indeed, the six already known pair correlations give an essentially exact limiting behavior of $\chi_\parallel^{\rm KIA}(T)$ for sufficiently large T, which allows an evaluation of $\Theta_{\rm CW}^{\rm KIA}$ that agrees exactly with Eq. (2.8). For the sake of completeness, we will derive it here and use it to verify the results of the high-temperature series expansion.

By adding a Hamiltonian $H_0 = -mh_z \sum_i \sigma_i^z$ corresponding to an applied longitudinal magnetic field h_z to Eq. (2.1), one can write

$$\langle \sigma_0^z \rangle = Z^{-1} Tr_\sigma \sigma_0^z e^{-\beta H} \tag{2.9}$$

where $H = H_0 + H_{\rm pair}$ and the partition function $Z = Tr_\sigma e^{-\beta H}$. Then it follows that the *initial isothermal parallel susceptibility* per site, $\chi_\parallel(T)$, becomes

$$\chi_\parallel(T) \equiv m \lim_{h_z \to 0} \frac{\partial \langle \sigma_0^z \rangle}{\partial h_z} = m^2 \beta \sum_i \langle \sigma_0^z \sigma_i^z \rangle_0, \tag{2.10}$$

where the subscript $\langle \cdots \rangle_0$ means the correlations are to be evaluated at $h_z = 0$. Thus, an exact calculation of $\chi_\parallel(T)$ at all temperatures requires the knowledge of temperature-dependent pair correlations at all distances. While this has not been possible as yet, it is clear from Fig. 2 that pair correlations that are farther in distance decay faster with increasing temperature. Thus, e.g., the unknown pair correlations at distances

TABLE I. Characteristics of the six pair correlations $\langle ij\rangle$, in increasing order of the distance between sites i and j given in units of the lattice spacing a. Site numbers refer to Fig. 1. NEP refers to the number of equivalent pairs obtained from Fig. 1 by keeping one site fixed at the origin and counting all sites at the same distance that are geometrically equivalent. Note that pairs $\langle 15\rangle$ and $\langle 06\rangle$ are at the same distance, but their environments are different.

Pair	Distance	Neighbor	NEP
$\langle 01\rangle$	a	1st	4
$\langle 05\rangle$	$\sqrt{3}a$	2nd	4
$\langle 15\rangle$	$2a$	3rd	2
$\langle 06\rangle$	$2a$	3rd	4
$\langle 16\rangle$	$\sqrt{7}a$	4th	8
$\langle 26\rangle$	$3a$	5th	4

larger than three lattice spacings will become negligible at temperature $1/|4Q_2| \gg 2$. As far as the high-temperature results are concerned, we can therefore expand $\chi_\parallel(T)$ in a series with increasing distance between the sites so that the *reduced* parallel susceptibility, using Eq. (2.6), is given by

$$\frac{\chi_\parallel^{\rm KIA}(T)}{\chi_2^0} = q\beta|J_2|[1 + 4\langle 01\rangle + 4\langle 05\rangle + 2\langle 15\rangle + 4\langle 06\rangle + 8\langle 16\rangle + 4\langle 26\rangle + \cdots], \quad (2.11)$$

where the coefficients are the number of equivalent pairs at the same distance, as shown in Table I. As Fig. 2 shows, this series converges very rapidly since the correlations become smaller, especially at high temperatures.

Figure 4 shows the inverse parallel susceptibility $(\chi_\parallel^{\rm KIA}/\chi_2^0)^{-1}$ for KIA as the number of pair correlations included in the evaluation is increased from the nearest four (up to the 3rd nearest neighbor) to the nearest six (up to the 5th nearest neighbor) pair correlations. As Table I shows,

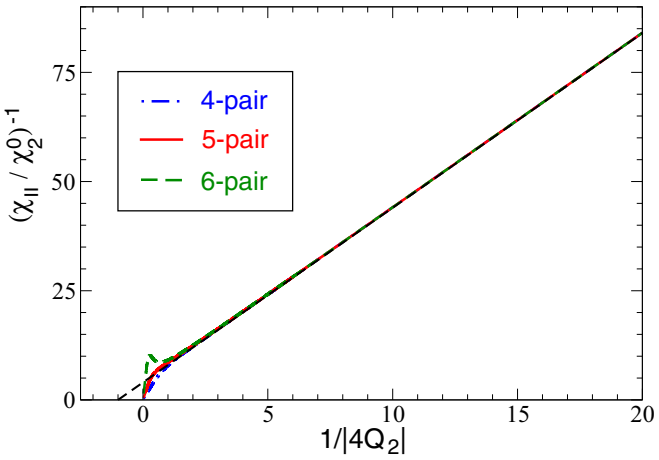

FIG. 4. Inverse of the reduced parallel susceptibility [Eq. (2.11)] as a function of reduced temperature [Eq. (2.7)] for KIA including four, five, and six pair correlations. As the number of pair correlations is increased from four to six, the low-T results fluctuate but the high-T behavior converges rapidly. The dashed (black) line extrapolated from high temperature gives $\Theta_{\rm CW}^{KIA} = 4J_2/k_B$.

this corresponds to increasing the distance around the origin from one lattice site up to three lattice sites. Clearly, the low-T behavior keeps on changing with addition of further correlations, but the high-T behavior converges rapidly; indeed, adding the sixth pair $\langle 26\rangle$ to the series truncated at the fifth pair $\langle 16\rangle$ does not appreciably change the result beyond $1/|4Q_2| \gg 5$; the fractional change at $1/|4Q_2| = 10$ is $\sim$0.006%, and at $1/|4Q_2| = 30$ it is $\sim$0.0002%, the convergence being progressively better at higher temperatures. However, to keep the low-T fluctuations clearly visible, we show the results only up to $1/|4Q_2| = 20$ in Fig. 4. Thus the high-T limiting behavior shown in Fig. 4 is essentially exact; the extrapolation of this high-T result gives the Curie-Weiss temperature $\Theta_{\rm CW}^{\rm KIA} = 4J_2/k_B$, which agrees with the high-temperature expansion of [32] given by Eq. (2.8) with $q = 4$. For comparison, we note that for TIA, $\Theta_{\rm CW}^{\rm TIA} = 6J_2/k_B$, the difference being the lattice coordination number. As we will see later, a finite (nonzero) x-axis intercept $\Theta_{\rm CW} < 0$ is a signature of frustration, but the magnitude itself depends on the lattice coordination number and is not necessarily a measure of the strength or degree of frustration. As we will show in the next section, the triplet interaction model leads to $\Theta_{\rm CW} = 0$, implying zero geometrical frustration. Note that for ferromagnets, the high-temperature extrapolation leads to a positive $\Theta_{\rm CW}$ which also corresponds to zero frustration.

III. KAGOME ISING ANTIFERROMAGNET WITH TRIPLET INTERACTION (KIA-T)

The Hamiltonian of the two-dimensional Ising antiferromagnet KIA-T with triplet interactions around elementary triangles on a kagome lattice is defined as

$$H_{\rm triplet} = -J_3 \sum_\tau \sigma_i\sigma_j\sigma_k, \quad (3.1)$$

where for notational simplicity we have omitted the superscript z on the Pauli spin operators by replacing them with the isomorphic Ising variables $\sigma_s = \pm 1$. Here $\sum_\tau$ designates summation over all elementary triangles and we consider the antiferromagnetic case for the triplet interaction $J_3 < 0$. This is an example of a spin model on a lattice with elementary triangles but without frustration. For example, each spin in a $(+,+,-)$ configuration on a triangle is "satisfied"; flipping any one would increase the energy.

The model (3.1) belongs to a class of Ising models having specific multispin ("cluster") interactions of only one kind and whose partition functions are easily and exactly calculable [34]. The calculational simplicity is recognized in the diagrammatic expansion of the partition function in powers of $\tanh Q$ ($Q = \beta J$ being an appropriate dimensionless interaction parameter), where no finite length path consisting exclusively of basic interaction clusters can totally close upon itself, thus only the path of zero length contributes to the partition function in the thermodynamic limit. Solutions for multispin correlations can similarly be determined exactly in these specific Ising models.

In Ref. [34], the partition function as well as all multisite correlations of a four-spin interaction model in a three-dimensional pyrochlore lattice were obtained by exploiting the nature of lattice graphs of corner-sharing tetrahedra.

Because the kagome lattice is also corner sharing, it is possible to adapt the same graph-theoretic techniques for a two-dimensional kagome lattice and obtain exact results for the triplet interaction model (3.1). In both cases, due to the facts that $\sum_{\sigma_p=\pm1}\sigma_p^{2n+1}=0$ and $\sum_{\sigma_p=\pm1}\sigma_p^{2n}=2$ for $n=0,1,2,\ldots$, the partition function sum over all possible spin configurations yields only two terms associated with simple complimentary lattice graphs, viz., totality of triangles being "unshaded" and totality of triangles being "shaded" (see Ref. [34] for three-dimensional analog). The resulting partition function Z_N for an N-site kagome lattice becomes

$$\begin{aligned} Z_N &= \sum_{\sigma} e^{Q_3\sum_\tau \sigma_i\sigma_j\sigma_k} \\ &= (\cosh Q_3)^{2N/3}\sum_{\sigma}\prod_{\tau}(1+\sigma_i\sigma_j\sigma_k\tanh Q_3) \\ &= (\cosh Q_3)^{2N/3}2^N[1+(\tanh Q_3)^{2N/3}], \end{aligned} \tag{3.2}$$

imposing periodic boundary conditions. Here the dimensionless interaction parameter Q_3 is defined in the same way as in Eq. (2.3), namely,

$$Q_3 \equiv \beta J_3. \tag{3.3}$$

This partition function differs from the four-spin interaction pyrochlore model [34] only by the exponent $2N/3$, which is the number of elementary triangles in a kagome lattice. Using Eq. (3.2), it follows that for $T\neq 0$,

$$\begin{aligned} -\beta f(Q_3) &= \lim_{N\to\infty}\frac{1}{N}\ln Z_N(Q_3) \\ &= \frac{2}{3}\ln\cosh Q_3 + \ln 2 = \ln[2(\cosh Q_3)^{2/3}], \end{aligned} \tag{3.4}$$

where $f(Q_3)$ is the magnetic Helmholz free energy per spin. This will be used to calculate the entropy per site later in Sec. III C.

A. Perpendicular susceptibility

Following [31], the exact perpendicular susceptibility per site can be written as

$$\chi_\perp = m^2\beta\left\langle\frac{\tanh[Q_3(\sigma_1\sigma_2+\sigma_3\sigma_4)]}{Q_3(\sigma_1\sigma_2+\sigma_3\sigma_4)}\right\rangle. \tag{3.5}$$

The argument within the thermal average can be expanded as

$$\frac{\tanh[Q_3(\sigma_1\sigma_2+\sigma_3\sigma_4)]}{Q_3(\sigma_1\sigma_2+\sigma_3\sigma_4)} = B^+ + B^-\sigma_1\sigma_2\sigma_3\sigma_4, \tag{3.6}$$

where the parameters $B^\pm$ can be obtained as follows: Using spin configurations where the spin products are all positive, one obtains $\tanh[2Q_3]/2Q_3 = B^+ + B^-$, while for spin configurations in which the product $\sigma_1\sigma_2$ has opposite sign to the product $\sigma_3\sigma_4$ one finds $1 = B^+ - B^-$. The solutions are

$$B^\pm = \frac{1}{2}\left[\frac{\tanh 2Q_3}{2Q_3}\pm 1\right]. \tag{3.7}$$

The thermal average of four spins in the "bow-tie" unit $\langle\sigma_1\sigma_2\sigma_3\sigma_4\rangle$ (see Fig. 1) can be obtained as follows:

$$\begin{aligned} \langle\sigma_1\sigma_2\sigma_3\sigma_4\rangle &= \frac{1}{Z_N}\sum_\sigma \sigma_1\sigma_2\sigma_3\sigma_4\, e^{Q_3\sum_\tau\sigma_i\sigma_j\sigma_k} \\ &= \frac{1}{Z_N}(\cosh Q_3)^{2N/3}\sum_\sigma \sigma_1\sigma_2\sigma_3\sigma_4 \\ &\quad\times\prod_\tau(1+\sigma_i\sigma_j\sigma_k\tanh Q_3). \end{aligned} \tag{3.8}$$

Again, the summation yields only two nonzero terms, and the result is

$$\begin{aligned} \langle\sigma_1\sigma_2\sigma_3\sigma_4\rangle &= \frac{1}{Z_N}(\cosh Q_3)^{2N/3}2^N[(\tanh Q_3)^2 \\ &\quad+(\tanh Q_3)^{2N/3-2}] \\ &= \tanh^2 Q_3, \end{aligned} \tag{3.9}$$

having substituted Eq. (3.2) and then letting $N\to\infty$. Hence, using Eqs. (3.5)–(3.7) and (3.9), the reduced perpendicular susceptibility per site becomes

$$\frac{\chi_\perp^{\text{KIA-T}}}{\chi_3^0} = \frac{q}{2}[|Q_3|(1-\tanh^2|Q_3|)+\tanh|Q_3|], \tag{3.10}$$

where we have defined the unit of susceptibility, similar to Eq. (2.6), as

$$\chi_3^0 \equiv \frac{m^2}{q|J_3|}. \tag{3.11}$$

One observes that results (3.4) and (3.10) are independent of the sign of Q_3, and so are valid for ferromagnetic interactions as well, an *a posteriori* justification for the absence of frustration.

It is interesting that result (3.10) for a three-spin interaction model on a kagome lattice in two dimensions is the same as for the four-spin interaction model on a pyrochlore lattice in three dimensions [34]. In Fig. 5, we show the inverse of the reduced perpendicular susceptibility for KIA-T, $[\chi_\perp^{\text{KIA-T}}(T)/\chi_3^0]^{-1}$, as a function of the reduced temperature

$$\frac{1}{|4Q_3|} = \frac{k_BT}{4|J_3|}. \tag{3.12}$$

In contrast to KIA shown in Fig. 3, it is finite at $T=0$. The kagome Ising ferromagnet, with long-range order below a critical temperature T_c, also has a finite value of the perpendicular susceptibility at zero temperature [31] and looks very similar to KIA-T. The signature for long-range order in $\chi_\perp(T)$ is the presence of a vertical inflection point at $T=T_c$. As shown in Fig. 5, $\chi_\perp^{\text{KIA-T}}(T)$ is devoid of any vertical inflection point.

B. Parallel susceptibility

As shown in Sec. II B, the parallel susceptibility per site requires only pair correlations, but at all distances. However, all pair correlations in the triplet model (3.1) vanish (see [34] for analogous graph-theoretic reasonings), so that Eq. (2.10)

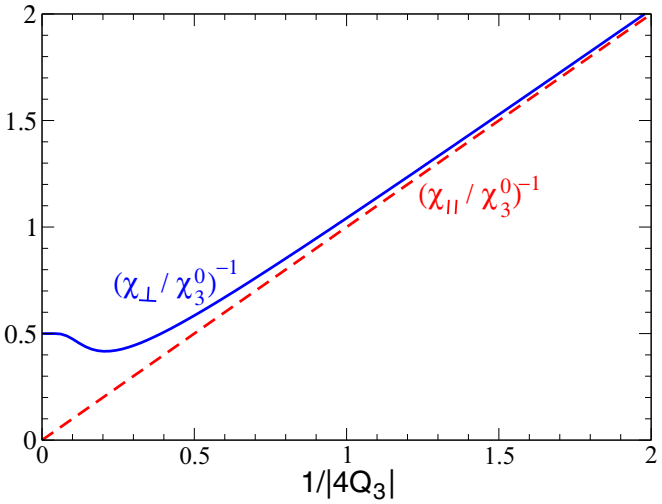

FIG. 5. Inverse of the exact reduced perpendicular susceptibility (3.10), solid (blue) curve, and parallel susceptibility [Eq. (3.13)], dashed (red) line, as a function of reduced temperature [Eq. (3.12)] for the triplet interaction model KIA-T. The absence of a $1/T$ divergence for $\chi_\perp^{\mathrm{KIA-T}}$ as $T \to 0$ as well as $\Theta_{\mathrm{CW}}^{\mathrm{KIA-T}} = 0$ implied by the zero intercept of $(\chi_\parallel/\chi_3^0)^{-1}$ are in clear contrast with the corresponding results for KIA shown in Figs. 3 and 4, respectively.

gives, using Eq. (3.11),

$$\frac{\chi_\parallel^{\mathrm{KIA-T}}}{\chi_3^0} = \frac{4|J_3|}{k_B T}. \tag{3.13}$$

For comparison, we add the inverse of the reduced parallel susceptibility as a function of the reduced temperature in Eq. (2.7) in Fig. 5. The result is a straight line through the origin, giving $\Theta_{\mathrm{CW}}^{\mathrm{KIA-T}} = 0$. This suggests a strong disorder, but without frustration.

C. Entropy

The partition function (3.2) can be used to calculate the entropy for the triplet model exactly. Using the expressions for the magnetic Helmholtz free energy F and the internal energy U in terms of the partition function and the relation $F = U - TS$, one obtains

$$S_N = k_B\left(1 - \beta\frac{\partial}{\partial\beta}\right)\ln Z_N. \tag{3.14}$$

In the thermodynamic limit $N \to \infty$, the entropy per site for KIA-T then becomes, using
Eqs. (3.4) and (3.14),

$$\begin{aligned}\frac{S^{\mathrm{KIA-T}}}{Nk_B} &= \beta^2\frac{\partial}{\partial\beta}f(Q_3)\\ &= \ln 2 + \frac{2}{3}[\ln(\cosh Q_3) - Q_3\tanh Q_3].\end{aligned} \tag{3.15}$$

The zero-temperature residual entropy is given by the $|Q_3| \to \infty$ limit leading to $S_0^{\mathrm{KIA-T}}/Nk_B = \ln 2 - (2/3)\ln 2 = (\ln 2)/3 = 0.231049\cdots$, which is finite but less than KIA or TIA. This is an example with no geometrical frustration but a large ground-state degeneracy. Thus a finite residual entropy is not necessarily a measure of the degree of frustration. We will argue below that a more appropriate measure of the degree of frustration arises from the consideration of the perpendicular susceptibility.

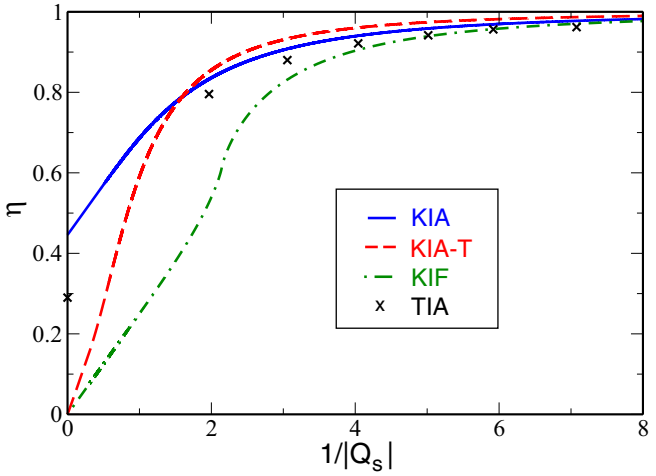

FIG. 6. Proposed frustration parameter $\eta(T)$, defined in Eq. (4.1), as a function of reduced temperature $1/|Q_s| = k_B T/|J_s|$, where $s = 3$ for triplet interaction model KIA-T and $s = 2$ for the other three cases with pair interactions, as listed in Sec. IV. For kagome ferromagnet shown by the dot-dashed (green) line, the transition temperature is characterized by a vertical inflection point at $1/|Q_2| = 2.14\cdots$. The others have no long-range order. The black crosses are calculated using sample data points for TIA obtained digitally from Fig. 7 of Ref. [30].

IV. DEGREE OF FRUSTRATION

We now define a quantity η derived from the perpendicular susceptibility as

$$\eta(T) \equiv \left(\frac{k_B T}{m^2}\right)\chi_\perp(T). \tag{4.1}$$

Figure 6 shows $\eta(T)$ for four different Ising models:

(i) Kagome Ising antiferromagnet (KIA): A model with strong geometrical frustration and no long-range order down to zero temperature, with finite residual entropy [29] $S_0^{\mathrm{KIA}}/Nk_B = 0.5018\cdots$.

(ii) Kagome triplet-interaction Ising model (KIA-T): A model with no geometrical frustration and no long-range order down to zero temperature, with finite residual entropy $S_0^{\mathrm{KIA-T}}/Nk_B = 0.2310\cdots$.

(iii) Kagome Ising ferromagnet (KIF, from [31]): A model with no frustration which develops long-range order below a finite critical temperature T_c and has zero residual entropy.

(iv) Triangular Ising antiferromagnet (TIA, from [30]): A model with strong geometrical frustration (but weaker than KIA) and no long-range order down to zero temperature. The residual entropy is finite [27,28], with $S_0^{\mathrm{TIA}}/Nk_B = 0.3231\cdots$.

As expected, all high-T results approach the $\eta(T \to \infty) = 1$ limit corresponding to free spins at thermal energies $k_B T$ much larger than interaction strength

parameters. We define the zero-temperature limit

$$\eta_0 \equiv \eta(T \to 0) \tag{4.2}$$

such that in the presence of a finite interaction between the spins, the point $\eta_0 = 1$ can be thought of as a limit of "maximum possible frustration," corresponding to all spins remaining fully frustrated down to $T = 0$. The opposite case of "no frustration" would correspond to $\eta_0 = 0$. This indeed is the case for all systems with long-range order below a finite $T = T_c$, as exemplified by case (iii) and has been shown exactly for the ferromagnetic kagome lattice [31] as well as the antiferromagnetic plane honeycomb lattice [35], all having a ground state with long-range order. For the three systems with finite residual entropy at $T = 0$, η_0 is larger for the kagome lattice $(0.4458\cdots)$ compared to the triangular lattice $(0.2900\cdots)$; the triplet interaction model with no frustration has $\eta_0 = 0$. Thus a clear feature emerges: the limiting value η_0 decreases with decreasing frustration. In other words, the parameter η_0 derived from the perpendicular susceptibility can provide a good measure of geometrical frustration in the state at $T = 0$. It is worth emphasizing that η_0 is essentially the amplitude of the $1/T$ divergence of $\chi_\perp(T)$ as $T \to 0$, so that $\eta_0 = 0$ implies the absence of any divergence.

We note that the two cases (ii) and (iii) with $\eta_0 = 0$ both have zero frustration, but not necessarily long range order at zero temperature. The signature of long range order in (iii) is a vertical inflection point for the kagome Ising ferromagnet (at $1/|Q_2| = 2.14\cdots$), which is absent in KIA-T. Thus $\eta_0 = 0$ does not necessarily imply a disordered ground state, it characterizes only the part of disorder due to geometrical frustration.

Similarly, case (ii) exemplifies the fact that there can be absence of long-range order down to zero temperature in an Ising system not only due to geometrical frustration but also due to, e.g., long-range or multiparticle interactions. This suggests that we distinguish between a "geometrically frustrated disordered state" characterized by $\eta_0 \neq 0$ with KIA and TIA as examples and a "disordered state with no frustration" characterized by $\eta_0 = 0$ with KIA-T as an example. Note that the triplet model KIA-T has a finite residual entropy, as do KIA and TIA, and therefore residual entropy does not distinguish between the finite and zero frustration cases.

V. SUMMARY AND DISCUSSION

In this work we have calculated exactly the perpendicular susceptibility of a KIA model and a triplet interaction model KIA-T. Both models lead to disordered ground states, but we make a distinction between disordered states with or without geometric frustration. By comparing the exact results obtained for KIA and KIA-T considered in this work with known exact results for TIA and the kagome ferromagnet, we argue that the quantity η_0 defined in Eq. (4.2), which is the amplitude of divergence of the perpendicular susceptibility at zero temperature, can be used as a quantitative measure of degree of frustration. We conclude that while geometric frustration prevents long-range order in TIA or KIA, Ising spin systems with no frustration can also lead, due to, e.g., multiparticle interactions, to states that remain disordered down to zero temperature. The longitudinal susceptibility provides an added insight into the difference between the two types of disorder, with the Curie-Weiss temperature being finite for disorder with frustration and zero for disorder without frustration.

Finally, we have considered separately a pair interaction model with geometrical frustration and a triplet interaction model with no frustration. While each has finite residual entropy implying large ground-state degeneracy, the nature of low-energy excitations in the two models is very different, as implied by the zero-temperature limits of the perpendicular susceptibility. In a more general case where both pair and triplet interactions are simultaneously present on a kagome lattice, the interplay of disorder with and without frustration may lead to more interesting possibilities. This is more than a mathematical curiosity, since the presence of a weak triplet interaction in addition to a dominant pair interaction is actually quite ubiquitous [36–40] in nature.

[1] See, e.g., review by A. P. Ramirez, Annu. Rev. Mater. Sci. **24**, 453 (1994).
[2] S. T. Bramwell and M. J. P. Gringas, Science **294**, 1495 (2001).
[3] C. Castelnovo, R. Moessner, and S. L. Sondhi, Nature **451**, 42 (2008).
[4] See, e.g., review by L. Balents, Nature **464**, 199 (2010).
[5] M. J. Harris, S. T. Bramwell, D. F. McMorrow, T. Zeiske, and K. W. Godfrey, Phys. Rev. Lett. **79**, 2554 (1997).
[6] S. H. Lee, C. Broholm, W. Ratcliff, G. Gasparovic, Q. Huang, T. H. Kim, and S.-W. Cheong, Nature **418**, 856 (2002).
[7] V. Fritsch, J. Hemberger, N. Buttgen, E.-W. Scheidt, H.-A. Krug von Nidda, A. Loidl, and V. Tsurkan, Phys. Rev. Lett. **92**, 116401 (2004).
[8] D. Bergman, J. Alicea, E. Gull, S. Trebst, and L. Balents, Nat. Phys. **3**, 487 (2007).
[9] See, e.g., H. T. Diep, *Frustrated Spin Systems*, 2nd ed. (World Scientific, Singapore, 2013).
[10] R. Moessner and J. T. Chalker, Phys. Rev. B **58**, 12049 (1998).
[11] R. Moessner and S. L. Sondhi, Phys. Rev. B **63**, 224401 (2001).
[12] H. J. Liao, Z. Y. Xie, J. Chen, Z. Y. Liu, H. D. Xie, R. Z. Huang, B. Normand, and T. Xiang, Phys. Rev. Lett. **118**, 137202 (2017).
[13] S. Yan, D. A. Huse, and S. R. White, Science **332**, 1173 (2011).
[14] S. Depenbrock, I. P. McCulloch, and U. Schollwock, Phys. Rev. Lett. **109**, 067201 (2012).
[15] Y. Iqbal, F. Becca, S. Sorella, and D. Poilblanc, Phys. Rev. B **87**, 060405 (2013).
[16] S. Jiang, P. Kim, J. H. Han and Y. Ran, arXiv:1610.02024.
[17] S. Nishimoto, N. Shibata, and C. Hotta, Nat. Comm. **4**, 2287 (2013).
[18] S. Yamaki, K. Seki, and Y. Ohta, Phys. Rev. B **87**, 125112 (2013).
[19] T. Yokota, Phys. Rev. E **89**, 012128 (2014).
[20] F. M. Zimmer, C. F. Silva, S. G. Magalhaes, and C. Lacroix, Phys. Rev. E **89**, 022120 (2014).
[21] M. Schmidt, C. V. Morais, and F. M. Zimmer, Phys. Rev. E **93**, 012147 (2016).

[22] L. Cano-Cort'es, A. Ralko, C. F'evrier, J. Merino, and S. Fratini, Phys. Rev. B **84**, 155115 (2011).
[23] O. Rojas, S. M. de Souza, and N. S. Ananikian, Phys. Rev. E **85**, 061123 (2012).
[24] R. Moessner, S. L. Sondhi, and P. Chandra, Phys. Rev. Lett. **84**, 4457 (2000).
[25] G. Misguich, C. Lhuillier, B. Bernu, and C. Waldtmann, Phys. Rev. B **60**, 1064 (1999).
[26] J. T. Chalker and J. F. G. Eastmond, Phys. Rev. B **46**, 14201 (1992).
[27] G. H. Wannier, Phys. Rev. **79**, 357 (1950).
[28] R. M. F. Houtappel, Physica (Amsterdam) **16**, 425 (1950).
[29] K. Kano and S. Naya, Prog. Theor. Phys. **10**, 158 (1953).
[30] J. Stephenson, J. Math. Phys. **5**, 1009 (1964).
[31] J. H. Barry and M. Khatun, Phys. Rev. B **35**, 8601 (1987).
[32] M. F. Sykes and I. J. Zuker, Phys. Rev. **124**, 410 (1961).
[33] J. H. Barry and M. Khatun, Int. J. Mod. Phys. B **11**, 93 (1997).
[34] J. H. Barry and F. Wu, Int. J. Mod. Phys. B **03**, 1247 (1989), and references cited therein.
[35] M. E. Fisher, Physica (Amsterdam) **26**, 618 (1960).
[36] M. W. Pestak, R. E. Goldstein, M. H. W. Chan, J. R. de Bruyn, D. A. Balzarini, and N. W. Ashcroft, Phys. Rev. B **36**, 599 (1987).
[37] B. M. Axilrod and E. Teller, J. Chem. Phys. **11**, 299 (1943).
[38] N. S. Sullivan, Bull. Magn. Reson. **11**, 86 (1989), and references cited therein.
[39] M. Roger, J. J. Hetherington, and J. M. Delrieu, Rev. Mod. Phys. **55**, 1 (1983).
[40] J. H. Barry and N. S. Sullivan, Int. J. Mod. Phys. B **07**, 2831 (1993).